Longshore transport gradients and erosion processes along the Ilha Comprida (Brazil) beach system

Filipe Galiforni Silva[1] · Paulo Henrique Gomes de Oliveira Sousa[2] · Eduardo Siegle[2]

Abstract The aim of this study is to assess the longshore transport gradients and wave power distribution along the Ilha Comprida beach system and relate it to the distribution of the current erosion process along this barrier island. The study is based on quantitative analysis of the potential longshore drift and the wave power distribution, as well as on the morpho-sedimentary seasonal variations in the beach system. Therefore, the 30-year wave reanalysis database from the global wave generation model WAVEWATCH III (NOAA/NCEP) has been extracted and analyzed for the region, as well as field surveys with topographic measurements and sediment samples. The numerical model MIKE 21 SW has been applied to propagate waves onshore and recognize the longshore transport tendencies and the nearshore wave power distribution. Results show an overall transport trend to the NE, being larger in the southern sector than in the northern sector of the island. Varying transport magnitudes prove to generate gradients in longshore drift. Two positive gradients in the longshore drift, resulting in local sediment losses, are observed. One is found in the central-southern area and another in the northern part of the island. Both areas coincide with erosive spots, as observed through field surveys. The central-southern positive gradient becomes larger and

migrates to the south during the most energetic months, while the northern gradient presents only variations in magnitude, being relatively stable in position throughout the year. Nearshore wave power results show two main areas with higher values that coincide with the positive longshore transport gradients. Sediment data presents low temporal variability, although spatial variations have been found reflecting the local hydrodynamic conditions, while the volumetric data shows largest values in the central-northern sector, being smaller in the central-southern and northern regions. Moreover, the central portions are more stable than the extreme portions regarding its seasonal variability. Our findings show that along this wide open stretch of coastline, exposed to the same offshore wave regime, an alternated nearshore wave regime results in areas with hydrodynamic conditions which lead to erosion or accretion. Erosion is caused by negative sediment balance as a function of higher wave power and positive gradients in longshore transport, and accretion due to lower wave power and negative gradients in longshore transport. Our findings help in further understanding the island's long-term evolution and current state of its beaches.

Keywords Longshore transport · Barrier island · Coastal erosion

✉ Eduardo Siegle
  esiegle@usp.br

1 Water Engineering and Management, University of Twente, P.O. Box 217, 7500 AE Enschede, The Netherlands

2 Instituto Oceanográfico, Universidade de São Paulo, Praça do Oceanográfico, 191, 05508120 São Paulo, Brazil

1 Introduction

Coastal erosion is a problem which affects, at different temporal and spatial scales, most of the coastal regions around the world. Estimates indicate that about 70 % of the world's coastlines are retreating (Davis Jr and Fitzgerald 2004; Bird 2008), due to natural or human-induced processes (Cai et.al. 2009). Complex processes acting at various time and space scales result in shoreline changes (Stive et al 2002; Miller and

Dean 2004). In this sense, seasonal variations may be important in explaining coastal variability (Komar 1998) as well as inter-annual forcing (e.g. Pianca et al 2015).

In order to better manage coastal areas, it is of prime importance to understand the processes that lead to coastal erosion and shoreline changes. One of such processes is the longshore drift pattern. Due to approaching wave patterns and coastline orientation, gradients in longshore sediment transport may be generated and, considering the mass conservation, positive gradients may result in shoreline retreat and negative gradients in shoreline accretion. In this sense, Bittencourt et al. (2005) found relations between negative and positive transport residuals and shoreline changes for a northern region of the Brazilian coast. Georgiou and Schindler (2009) verified the influence of longshore drift gradient trends and wave energy distribution in the recent evolution of the Chandeleur Islands (USA), addressing an important seasonal contribution to its actual development. In a long-term perspective, Siegle and Asp (2007) and Martinho et al. (2009) related transport gradient trends to barrier evolutionary aspects and coastal infilling processes during the Holocene period. Therefore, the assessment of the longshore transport gradients can drive a first-order approximation of vulnerable regions to shoreline changes due small alterations on the adjacent system (e.g., sediment input, terrain subsidence) and explain recent erosional patterns.

Ilha Comprida is a 65-km-long exposed barrier island located in the south of São Paulo's state coast which is presenting punctual erosional characteristics. The barrier (Fig. 1) is composed mainly by quaternary fine and very fine sands (Tessler 1988), with width ranging between 0.5 and 5 km, being limited by two inlets: Icapara inlet at north and Cananéia inlet at south (Guedes et al. 2011). Although being understudied, both inlets present ebb-tidal delta systems, being the one located at the Cananéia inlet the most prominent. Furthermore, both are influenced by the opening of an artificial channel called Valo Grande, which connects the Ribeira de Iguape River to the inner lagoon and became a source of fresh water and sediments into the system (Conti et al. 2012).

The region is controlled by nearshore currents generated through approaching deep-sea waves, which has its incidence and energy patterns related to the occurrence of frontal systems. These Atlantic meteorological systems generate winds coming from the east and south, making the incoming waves a direct response of the winds at the sea (Araújo et al. 2003). At the Brazilian southeastern region, the meteorological events are characterized by the dominant change of two main air-mass: the tropical air-mass called South Atlantic Tropical Anticyclone (ATA), which is responsible for the trade winds throughout the year, therefore generating waves from the NE and E, and the polar air-mass called Atlantic Migratory Polar Anticyclone (APM), preceded by the frontal systems, thus resulting in waves from SE, S, and SW (Santos 2005). Due the shoreline orientation, the waves from S and SE produce longshore drift toward NE, while the waves from NE and E produce longshore drift toward SW (Tessler 1988; Pianca et al. 2010). The tidal regime is predominantly semi-diurnal and described as microtidal (tidal range lower than 2 m), with an average variation of 1.2 m during spring tide and 0.25 m during neap tide (Mesquita and Harari 1983; Harari and Camargo 1994).

Souza e Suguio (1996) characterized two main erosional stretches along the beach system of Ilha Comprida (SP, Brazil): one located in the central-southern region of the island and one located at the northern region of the island, both primarily associated to longshore drift divergence (Souza 1997). However, Sousa (2013), studying vulnerability indexes for coastal zone, evaluated the wave power distribution and longshore drift estimates for the entire island considering only the month with the highest cold front occurrence, recognizing the possibility of a contribution of the wave power together with the longshore patterns for the development of the erosional spots. Nonetheless, Sousa (2013) estimates did consider neither the seasonal variability nor the general tendencies from both, wave power and longshore drift, not taking into account the recovery processes involved and the real tendencies in a long-term analysis. Moreover, previous studies do not present any quantitative information about longshore drift patterns along the island, which is an important factor for the comprehension of the erosional processes and its variation at different time-scales. In a seasonal perspective, Marquez (2010) assessed the short-term morphological and volumetric variability of a beach stretch at the southern region of the island, recognizing wave patterns which contributed to the erosional process or sediment buildup. However, it is unclear if the other sectors of the island follow the same morphological variation pattern related to the same incoming waves. Therefore, the aim of this work is centered in recognizing the longshore drift gradients and the wave power distribution along the Ilha Comprida beach system, following the hypothesis that they relate directly to the shoreline change patterns and erosional spots along the island. The seasonal morpho-sedimentary variations are also used in order to help in better understanding the dynamics of this beach.

2 Data and methods

2.1 Wave data

Since no measured wave database is available for the region, the 30-year wave reanalysis database from the CFSR Reanalysis Hindcasts simulation has been used. This
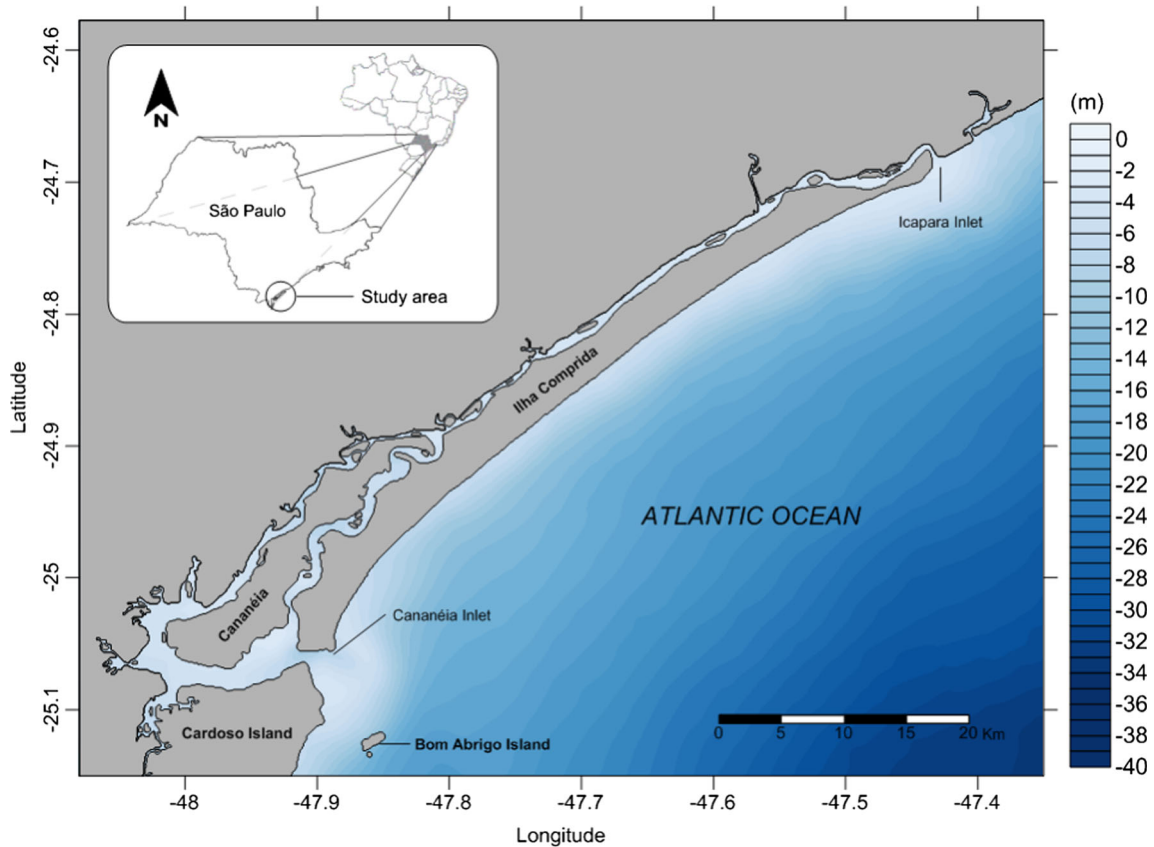
Fig. 1 Location of the study area

information is derived from the global wave generation model WAVEWATCH III (NOAA/NCEP—http://polar.ncep.noaa.gov/waves/CFSR_hindcast.shtml). This data was extracted at 26° S and 45° W, being statistically treated considering the range between $-3\sigma \leq \bar{\Upsilon} \leq 3\sigma$, where σ is the standard deviation and $\bar{\Upsilon}$ is the mean of the entire data set regarding each wave characteristic separately. After that, the data was analyzed by simple statistics, frequency table, and directional histogram, defining the region wave climate following the pattern shown in Pianca et al. (2010). Although presenting limitations when compared to in situ measured data, hindcasts from global wave generation models have been validated and shown to reproduce well the overall wave climate (e.g., Wang and Swail 2001; Tolman et al. 2002; Caires et al 2004). For southern Brazil offshore waters, Pianca et al. (2010) made a qualitative validation comparing WAVEWATCH III outputs with measured data. The authors showed that although the model slightly overestimates the occurrence of higher waves, the overall wave climate is well represented by the model estimates. Such differences are similar to those found by Tolman et al. (2002), which concluded that WAVEWATCH outputs overestimate wave heights by about 10 %, when comparing it to several buoy measurements.

2.2 Numerical modeling

Using the extracted wave information as boundary conditions, a nearshore wave transformation model has been applied in order to propagate the waves to nearshore. The applied model is the Spectral Wave module of MIKE 21 (developed by DHI). The model includes refraction, shoaling, and breaking, using the derivation of basic equations based on a parameterization of the wave action conservation equation, following the approximations described by Holthuijsen (1989). The wave parameters used as boundary conditions are the significant wave height (Hs), peak wave period (Tp), mean wave direction (°), and directional standard deviation (DSD). To summarize the model input data without representative loss, scenarios based on the occurrence percentage above 5 % regarding the Hs and related direction were considered. Wave period has been defined through the most frequent peak period related to each of the defined significant wave height and direction combination. Thereby, 80 simulations have been defined and run considering the entire data set and its seasonal division.

The area of interest lies well inside the model domain, with boundaries being approximately 100 km away. The coastline used in the model was extracted from georeferenced satellite images, while the bathymetry was processed from the global

model ETOPO1 and Navy charts. The flexible mesh which defines the grid was built with a gradual density increment toward the area of interest.

The nearshore wave characteristics for each scenario were extracted at depths of around 5 m, being used as a proxy of nearshore wave characteristics to estimate the longshore drift and wave power, relativized to their frequency of occurrence.

2.3 Potential longshore drift

Potential longshore drift estimates consider that (a) the wave energy is directly proportional to the square of its height (Davies 1980) and b) the intensity of the longshore drift is proportional to the angle with which the wave-front approaches the coast (Zenkovich 1967; Komar 1998), as given by

$$x = H^2 \sin\alpha \cos\alpha \qquad (1)$$

where α is the orthogonal coastline incidence angle, H is the nearshore wave height (in the present case waves along the 5-m isobaths), and x is the dimensionless longshore drift intensity. This method has been successfully applied by many researchers (Bittencourt et al. 2002; Bittencourt et al 2005; Siegle and Asp 2007; Cassiano and Siegle 2010; Sousa 2013), being considered appropriate for the aim of this study.

2.4 Wave power

The wave power is a parameter that considers the synergistic effect of both wave period and wave height and may be correlated with beach volume and stage variations (Short 1978). According to the linear wave theory, as exposed in Holthuijsen (2007), the wave energy flux is defined by the product of its energy per unit of area and the wave group velocity. Therefore, we can estimate the value through Eq. 2:

$$P = \frac{\rho g^2 H^2 T}{32\pi} \qquad (2)$$

where ρ is the water density (1027 kg/m³), g is the gravity acceleration (9.8 m/s²), H is the local wave height, in meters, and T is the period in seconds.

2.5 Morphological and sediment surveys

To recognize the morphological seasonal variations along the beaches that form the island, elevation surveys using Differential Global Positioning System (DGPS—Trimble 5700 and R4) have been carried out at five beach stretches. Surveys have been conducted during 1 year at a 3-month frequency (Fig. 2). Each surveyed stretch is 300 to 500 m long. All the measurements have been carried out during

low spring tides, thus leading to a larger coverage area. For each survey, grids were interpolated (Krigging method) and used for volume estimations and altimetry maps. For comparison purposes, each grid was limited transversally considering the minor width from the dataset, using the most landward foredune position of the time-series, for each sector, as a baseline. Furthermore, the volume values were divided by its length, thereby normalizing the data for spatial comparisons between the different stretches. Sediment samples were collected in the backshore and foreshore (face and terrace) for each sector during the different seasons and analyzed following the statistical method exposed in Folk and Ward (1957). Specific wave information for the surveyed period has been extracted from the global wave generation model WAVEWATCH III (NOAA/NCEP), using its standard output for the period.

2.6 Erosion assessment

Regarding the erosional process comprehension and considering the long-term data lack for the region, a geoindicator approach has been applied for a qualitative recognition of the current state of the erosion in the region, following the method proposed by Bush et al. (1999). This method proposes to identify spots of coastal erosion in a simple and fast way. Although the method proposes only a qualitative approach, it could be fairly used as a tool for first analysis in areas with low resources or data. To evaluate the existing erosional evidences in Ilha Comprida, criteria which consider areas without erosion evidence, with erosion evidence, and with severe erosion evidence were defined (Table 1).

3 Results

In order to analyze the results properly, the island has been divided in six main stretches regarding both the coastline orientation and regular coastline spacing (Fig. 2).

3.1 Wave climate

Waves from S, ENE, and SSW have been the most frequent throughout the 30 years analyzed, representing 60 % of the entire data set. The wave height of 1.5 m and period of 8 s have been the most frequent offshore wave pattern in the Brazilian southeastern region.

In a seasonal perspective, this pattern presents important variations in all wave properties. During summer, waves from ENE dominate the data set, with 28.5 % of the occurrence, followed by southerly waves with 17.8 % of occurrence. That pattern changes in autumn, with a direction switch of the dominant waves approaching from S and SSE with frequencies of 28.6 and 19.1 %,
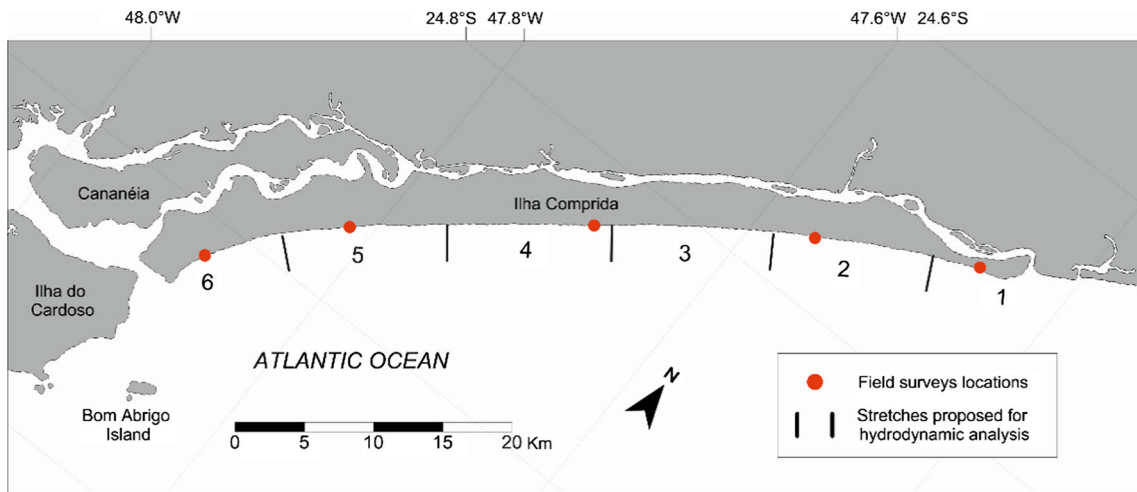
Fig. 2 Stretches defined for the erosion, longshore drift, and wave power data analysis. The *red circles* represent the field survey locations, being distinguished by the *stretch number*

respectively. During winter, wave climate is similar to that of autumn months, with the most frequent wave coming from S and SSE, with 27.4 and 21.4 %, respectively. In spring, the pattern changes, with most frequent waves coming from ENE, with 22.9 %, and S, with 21.0 %. Regarding the combined distribution of significant wave height and peak period, the most frequent wave pattern for the summer was 1.5 m and 8 s. Throughout the autumn, an increase in the period has been verified, located between 8 and 10 s, though the significant height has been the same as in the summer. In the winter months, two main high-frequency spots could be recognized: one related to waves with significant height of 1.5 m and peak period between 8 and 9 s and another related to waves with significant height of 2 m and peak period between 10 and 11 s. During the spring, waves at 1.5–2 m and 8–9 s predominate. The highest waves for each period are as follows: 5.59 m, with period of 12.7 s for summer; 6.8 m, with period of 13 s for autumn; 6.4 m, with period of 13 s for winter; and 6 m, with period of 11.9 s for spring. All these waves had their direction from SSW, with the one from spring being an exception, coming from S.

3.2 Potential longshore drift

Based on this offshore wave climate, the resulting potential longshore drift along the study region evidenced a general transport toward NE, with positive and negative gradient trends along the coastline (Fig. 3). Stretches 6 and 4 presented a longshore transport with values of 170 and 159, respectively, followed by sector number 5, with 134, and by the three remaining northward stretches 3, 2, and 1, with values of 80, 30, and 62. Positive gradient spots have been recognized between stretches 5-4, in the central-southern region of the island, and 2-1, in the northern region. The biggest gradient value has been found in the northern spot, with 34, while the central-southern gradient spot reaches values around 25. Both locations present erosional morphological indicators and characteristics of sediment loss in the beach-dune system. On the other hand, the regions between stretches 6-5, 4-3, and 3-2 presented negative gradient characteristics, resulting in large beach width and no erosion indication. The longshore residual convergence results presented values of around 36, 78, and 52, respectively, in the same locations cited above.

**Table 1** Coastal erosion classification procedures based on Bush et al. (1999)

	No erosion	Erosion	Severe erosion
Procedures for erosion classification	Vegetation presence and dunes without erosion signs	Scarps caused by waves in the foredune or backshore (high-energy events effect)	Absence of foredune and vegetation
	Beach wide with well-developed berm	Exposed vegetation roots in the foredune	Destruction of urban structure on beach or offshore
	Overwash absent, with no wave attack evidence in the foredune	Beach narrow or no high-tide beach	Active wave scarping of bluffs or dunes remnants
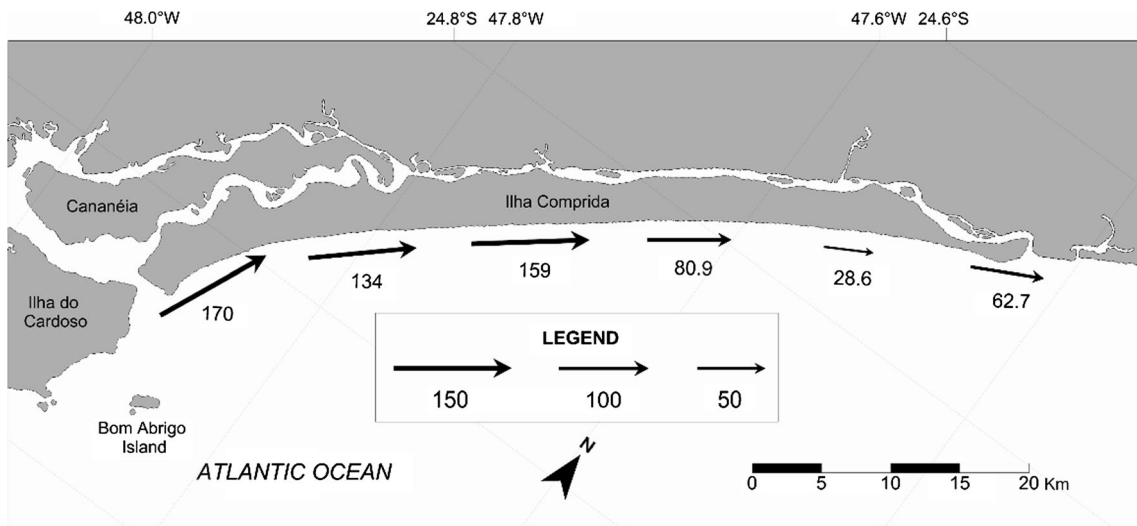
Fig. 3 Potential longshore drift distribution along the coast of Ilha Comprida, regarding the entire 30-year data set. The *values* are dimensionless

Seasonally, the potential longshore drift shows variations not only in magnitude but also in the resulting transport direction (Fig. 4). Throughout the summer, with incoming waves from ESE preferentially, the resulting transport has been oriented to SW, presenting two main positive gradient spots situated between stretches 4-3 and 2-1. In the autumn, a transport inversion toward NE could be recognized, with a spatial maintenance of the positive gradient spots. With the winter income, an intensification of the longshore drift toward NE is recognized, thus defining the period with higher transport values (up to 400). Other two important aspects should be highlighted in this season: an increase in the central-southern positive gradient zone toward southern regions (e.g., between 6-5 and 5-4) and the spatial maintenance of the northern positive

gradient between 1 and 2. The nearshore currents are smoothed with the spring arrival, causing a switch in the transport direction in sector number 6 to NE, presenting similar positive and negative gradient patterns than the summer period. Therefore, the northern positive gradient spot maintains its spatial position during all seasons, with a magnitude variation in the residual values, reaching greater levels during the spring (67) and summer (54), followed by autumn (38) and winter (36). On the other hand, the central-southern positive gradient region presents an increase in the acting area during the most energetic months toward southern regions, followed by a migration toward NE throughout summer. In a quantitative perspective, this sector presented higher residual divergence values when compared to the northern positive spot, being
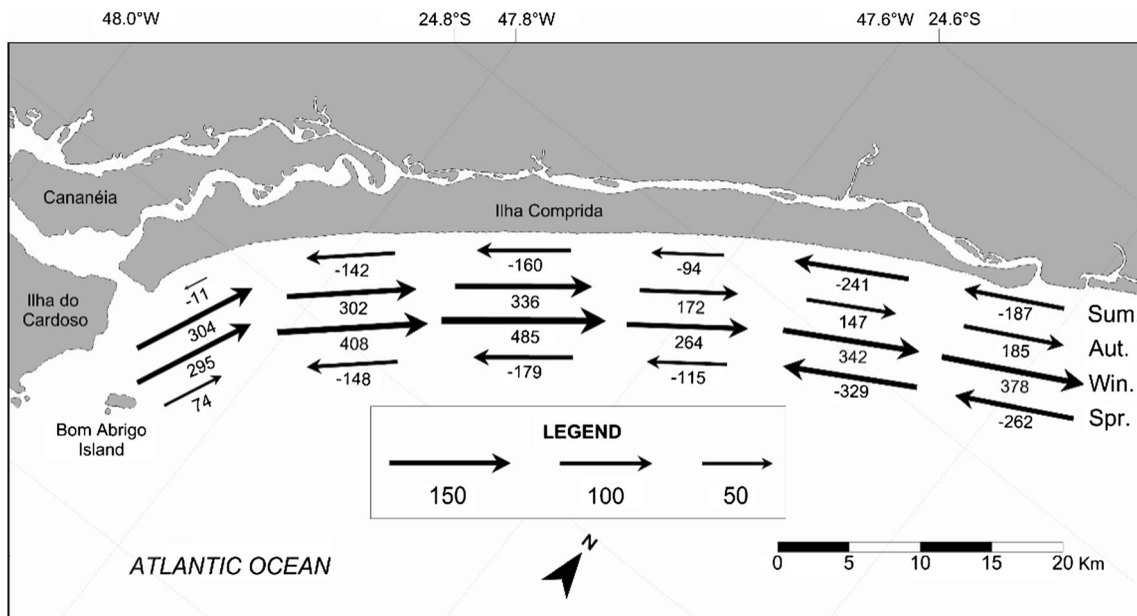
Fig. 4 Potential longshore drift along the coast of Ilha Comprida, regarding a seasonal distribution of the data set. The *values* are dimensionless

more prominent during the winter (103 between 6 and 5 and 77 between 5 and 4) than during the summer (66), spring (64), and autumn (34).

It is possible to notice a seasonal variability regarding the southern sector, which migrates toward SW in the most energetic months and toward NE during the summer, while the northern positive gradient spot maintains its position throughout the year. Moreover, the residual values in the northern spot are greater during the less energetic months, while in the central-southern divergence spot, the winter present the greatest values.
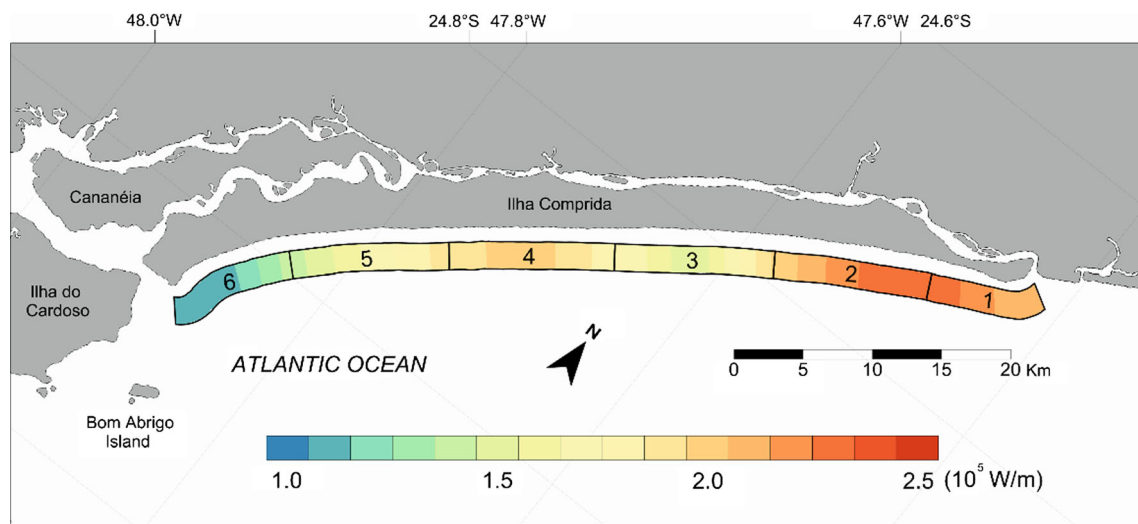
3.3 Wave power

The wave power results show a non-uniform energy distribution along the island, with minimum values of 100,000 W/m and maximum reaching 250,000 W/m approximately (Fig. 5). Spatially, two peaks are recognized, which are approximately the same as the longshore positive spots: one located between the 1–2 stretches and the other located near stretch number 4, with values reaching 220,000 W/m. The lower wave power levels are located near stretches 3 and 6, being the lowest one located in the most southern part of the island, with values of 100,000 W/m.

In a seasonality perspective, the spring and summer seasons presented milder conditions, with values not exceeding 220,000 W/m. However, during autumn and winter, the estimates may reach levels around 380,000 W/m due to the incoming energetic waves (Fig. 6). The two peak zones with the overall wave power concentration maintain their positions throughout the entire year. In the northern region, the zone which has been presenting the most important erosional problems and the spatial stable longshore positive gradient, the highest value of each season can be found. It means that the relative magnitude for each season suffers an important

variability, but the spatial maintenance of the two main wave power concentration spots leads to a stable non-uniform wave distribution along the coast (Fig. 7).

3.4 Erosion thematic map

The beach system is mostly dissipative with only small variations in its morphodynamic stages in the southern stretch (1), presenting intermediate to intermediate-reflective characteristics (Nascimento 2006). However, the beach system generally presents a large surf zone along the whole island. There are low height dunes which define the backshore limit virtually along the entire island. The results showed that the erosional or stable processes are well defined along all stretches, being classed as no erosion evidence areas at stretches 6, 3, and 2 and the southern region of stretch 5; erosion evidence areas at stretch 5 and the southern region of stretch 4; and severe erosion evidence areas at stretch 1 and the northern region of stretch 2 (Fig. 8). Areas without erosion evidences present vegetation along the foredune, a well-developed berm with large beach width. On the other hand, areas with erosion evidences are characterized by scarped dunes and foredune vegetation with exposed roots, while in the areas characterized with severe erosion evidences, there is absence of foredune and vegetation besides the destruction of urban structures such as houses, streets, etc. These results are consistent with those found by Souza and Suguio (1996), suggesting a spatial maintenance of the erosion and coastline stable processes. Moreover, these results corroborate with the social problems faced by the local population, mainly in stretch 1, where the coastline retreat is causing severe consequences.


Fig. 5 Wave power distribution along the coast of Ilha Comprida, considering the entire 30-year data set. The *values* are presented in Watts per minute
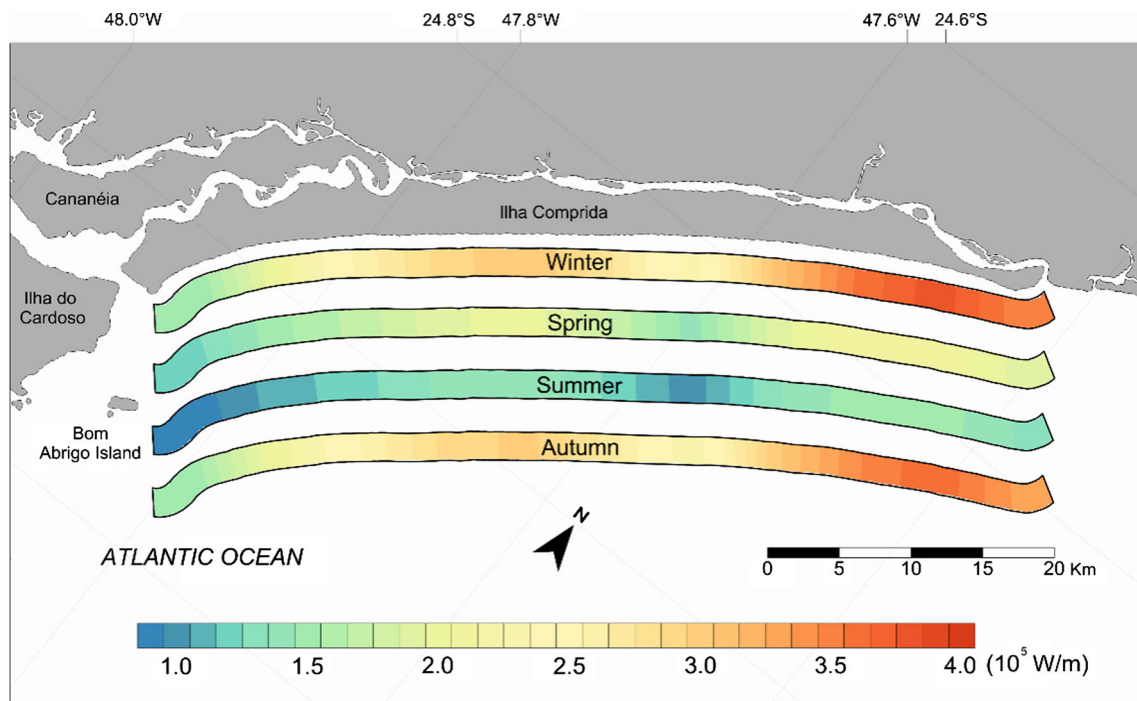
Fig. 6 Wave power distribution along the coast of Ilha Comprida, considering a seasonal distribution of the data set. The *values* are presented in Watts per minute

3.5 Morphological and sedimentary results

The results regarding the field surveys showed two main characteristics: the extreme island stretches present larger volume variability than the central stretches, and the sediment properties present low temporal variability, though spatial tendencies were recognized. The grain size distribution along the beach showed smaller grain size values
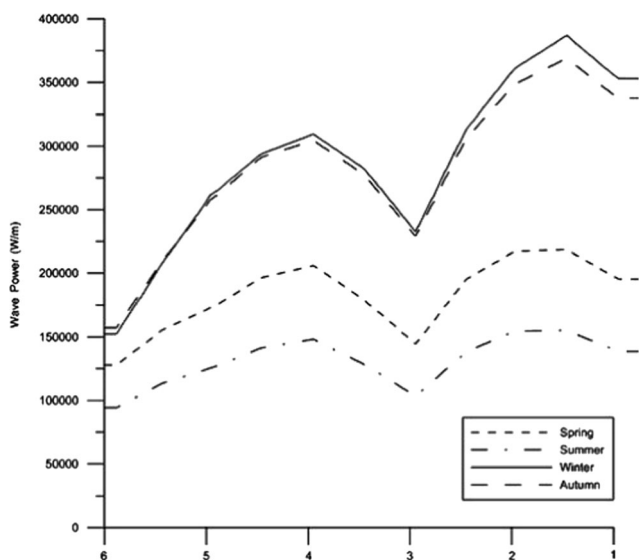

Fig. 7 Longitudinal section of each seasonal wave power distribution. The *y-axes* represent the wave power, in Watts per minute, while the *x-axes* represent the stretches of the island

in the northern portion (C1 and C2), while the larger values were found in stretches C5 and C6. Furthermore, the northern portion presented the lowest grain size standard deviation, coherent with its low temporal variability. The temporal grain size variability becomes higher towards the southern region, with ranges of up to 0.38 mm around stretch 6. The ebb-tidal delta might have great influence at this high variability not only in terms of wave attenuation but also in terms of sediment input due to shoal attachment processes. Regarding the sediment sorting, the largest values were found in the southern portion, with a reduction towards north. However, the northern portion presented lower temporal variation of sorting parameters when compared to southern stretches (Table 2). In relation to the skewness and kurtosis, all stretches present symmetric and mesokurtic sediment property distributions, with low temporal and spatial variability. This means that there is no tendency in the grain distribution to smaller or coarser grains and that it presents a normal distribution.

The volumetric data shows largest values in the central-northern sector, represented by stretches 2 and 4, with median values of 176 (10) and 173 (12) m^3/m, respectively, and the lowest values in the northern stretch 1 (approximately 140 m^3/m), as well as a standard deviation of almost 14 (Fig. 9). As in the grain size distribution, stretch 6 presented volume variations with time, with a standard deviation of 16 and a median value of about
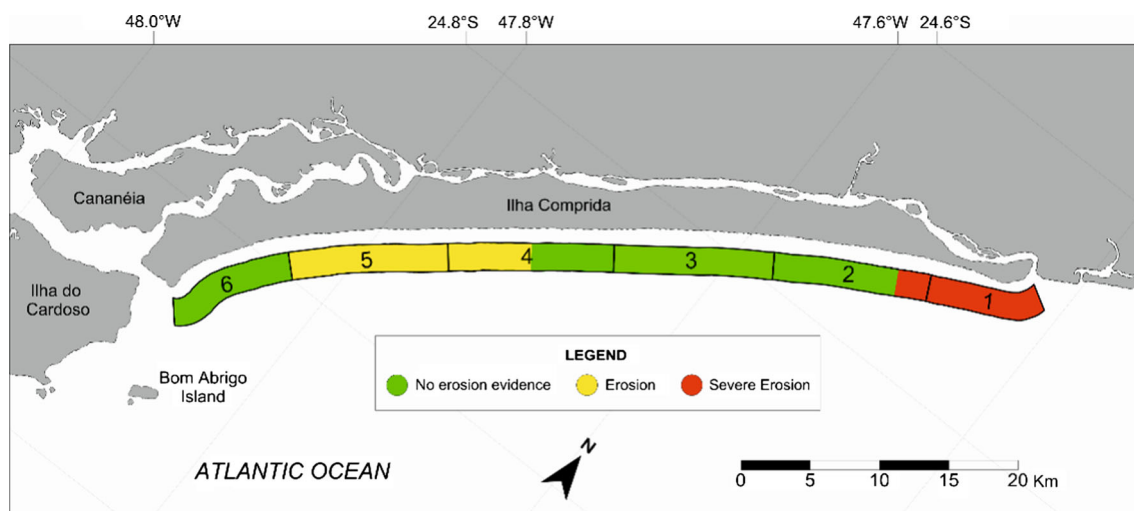
Fig. 8 Erosion thematic map built through geoindicators obtained during field expeditions, showing stretches with apparently severe erosion, erosion, and spots without erosional visible indicators during the experiment

150 m³/m. Stretch 5, which presents erosional characteristics, had median values of 142 m³/m and standard deviation of 8 m³/m. Although the values regarding stretches 1 and 5 are similar, the foredune scarp in the northern region retreated about 10 m comparing the first and the last survey, while the foredune in stretch 5 maintained approximately its position (Fig. 10). Moreover, stretch 1 presented a negative sediment balance of about 20 % in relation to the initial estimative, while stretch 5 presented a volume loss of about 1 % at the end of the surveyed period. Stretches 2 and 3 presented an accretion pattern of 5 and 8 %, respectively, and stretch 6 presented a negative volume balance of about 8 %. However, only stretches 1 and 4 presented final balance values which overcome the standard deviation.

The wave conditions for the survey period yield patterns for the volume variation analysis (Table 3). Stretches 2 and 4 responded equally regarding accretion and erosional patterns throughout the entire period. Furthermore, stretches 1 and 6 also responded similarly, though the erosional and accretion responses were out of phase when compared to the central

stretches during 2013. During 2014, all stretches responded in phase regarding accretion and erosional patterns.

4 Discussion

Sediments available at a beach are directly affected by processes that generate transport and change morphology at different scales. These processes act along the coast, transporting the sediment to different sectors laterally and across the coast removing sediments from the beach to the surf zone or vice versa (Siegle and Asp 2007; Van Rijn 2011). Therefore, the longshore transport processes approaching the beach can be related in a long-term analysis with potential erosion or accretion spots. Longshore drift divergence (or positive gradients) will result in erosion, while longshore drift convergence (or negative gradients) results in accretion (Stone et.al. 1992; Cipriani and Stone 2001; Bittencourt et al. 2005). Thereby, the results here presented indicate the direct relation between accretionary or erosive areas with negative and positive

Table 2 Grain statistical parameters along the different stretches

Sector	Grain size		Sorting		Assimetry		Kurtosis	
	Mean	Standard deviation	Mean	Standard deviation	Mean	Standard deviation	Mean	Standard deviation
C1	0.157	0.007	1.250	0.048	0.01	0.03	0.95	0.01
C2	0.154	0.008	1.259	0.044	0.02	0.04	0.96	0.01
C4	0.177	0.015	1.316	0.045	0.00	0.02	0.95	0.02
C5	0.214	0.020	1.368	0.058	−0.02	0.03	0.95	0.01
C6	0.219	0.038	1.435	0.160	−0.01	0.04	0.95	0.01

Values in millimeters
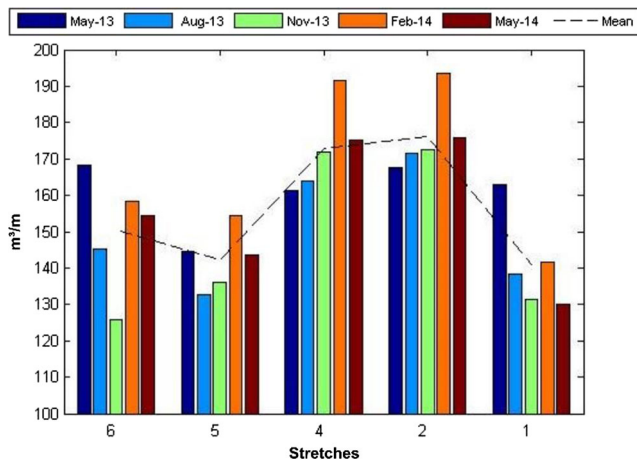
**Fig. 9** Normalized volume for each sector through all surveys

longshore drift patterns along the beach-dune system of Ilha Comprida (SP).

The island presents basically two potential erosional sectors: one located in the central-southern region (between stretches 5 and 4) and another located in the northern region (between stretches 2 and the entire 1). These regions are similar with those erosional spots found by Souza and Suguio (1996), indicating the spatial maintenance of the processes during the last decades. In the northern spot, the region which is characterized by severe erosion, a positive gradient

tendency of the longshore transport has been found, with greater values during summer and spring with a spatial stability throughout the year. On the other hand, in the central-southern spot, the region which also presents a positive gradient (in smaller magnitudes), the transport tendency suffers an apparent shift in its position, becoming higher and reaching further southern regions during the most energetic months. This spatial variability could affect the residual positive gradients in the area, once the central-southern positive gradient is spread longshore over a larger part of the coast, resulting in minor values per area unit, while the northern positive gradient acts in the same area throughout the year.

In addition to defining the magnitudes of longshore drift patterns, wave height variations along the coast define the amount of wave power a specific stretch of coast is subjected to. Our results also show that the wave power distribution has a spatial relation with the positive gradients in longshore drift, becoming an additional fact that combined to stronger longshore currents may have a synergistic effect on defining the erosional spots. The northern spot concentrates the greater value of wave power not only during the 30-year analysis but also in a seasonal perspective, always keeping its relative high levels when compared to other sectors of the island. The central-southern erosion spot also presents high relative wave power values, although at lower levels than the northern spot.

Fig. 10 Altimetry difference maps for stretches 1 (**a**) and 5 (**b**) (as indicated in Fig. 2). The *continuous red and black line* represents the foredune foot for the first and last survey, respectively. *Warm colors* represent sediment loss, while *cold colors* represent accretion
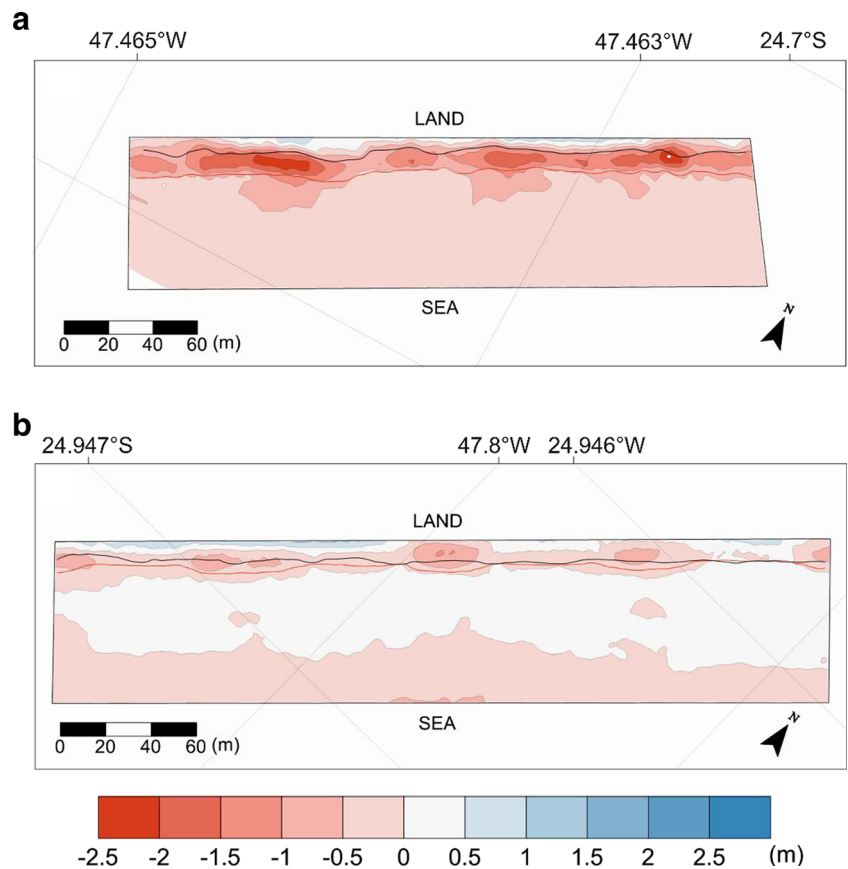
Table 3 Standard wave statistics and volume variation (%) throughout the survey period

Field	Hs	Tp	Dir	Hs	Tp	Dir	Volume variation (%)				
	3-Month period			Week prior the survey			1	2	4	5	6
May/13	1.9	9.4	148	2.3	9.1	161					
Aug/13	2.2	10.7	166	2.2	9.4	138	−25	4	3	−12	−23
Nov/13	2.5	9.1	127	3.2	10.8	186	−7	1	8	3	−19
Feb/14	2	8.3	119	1.8	6.5	66	10	21	20	18	33
May/14	1.9	7.8	124	2.1	8.1	131	−11	−18	−16	−11	−4
							20	**5**	**8**	**−0,7**	**−8**

The bold numbers in the volume variation column corresponds to the entire period balance (last survey-first survey)

Furthermore, no spatial migration of these high relative values has been found regarding seasonal aspects. Thereby, the wave power could have an important role in the erosional processes as the longshore gradients have, not only in a seasonal perspective as Short (1978) evaluated but also in a long-term analysis. High wave power values might have more capacity to reach the upper beach zone, withdrawing sediments from the foredune and backshore more frequently, thus making this material available for the longshore transport. Moreover, the Icapara inlet can be seen as a possible sink of sediments coming from stretch 1. A depositional process has been occurring in the region, with drastic morphological changes over the last four decades (Kawakubo 2009), with the sediment input through the artificial Valo Grande channel contributing to this process (Italiani e Mahiques 2014).

Besides the erosional spots, as a consequence of time and space variations of longshore drift gradients and wave power, the island also presents regions with negative longshore gradients and low wave power levels along its beach system. These regions are located in the central-northern sector (between stretches 4-3 and 3-2) and in the southern region (between stretches 6-5) and are characterized by wide beaches and large profile volumes, as confirmed by morphological surveys. Therefore, considering the northeasterly longshore transport tendency found on both sediment characteristics and numerical modeling results, the central-northern area can be defined as a sediment accumulation sector, with low wave power level and the converging residual longshore drift. This low energy depositional area may cause a reduction in the amount of sediment that is transported to the northern sectors that present a sediment deficit.

The longshore drift and wave power distribution have been strongly conditioned by the presence of the Bom Abrigo Island and the presence of the ebb-tidal delta on the Cananéia inlet, in the south, and overall by the coastline orientation (Fig. 1). Coastline orientation related to incident waves favors a longshore transport generated by waves from E and S, which reach the beach at angles closer to 45° intensifying longshore transport. However,

energetic waves incoming from SE which represents 18 % of occurrence have importance regarding the longshore drift only in the southern part of stretch 6, as a function of its coastline orientation. For the other stretches, waves from SE are more important regarding the transport across the coast, probably making upper beach sediments available for the longshore transport in the surf and swash zone. The Bom Abrigo Island and the presence of the ebb-tidal delta at the Cananéia inlet act, dissipating the wave energy that comes from S-SE on the southern region of stretch 6, reducing its influence towards central and northern portions.

Considering the wave climate and beach response in the extreme portions, the erosion process could be expected in a long-term tendency. Waves with these erosional characteristics have been more frequent not only in the entire analysis period, corresponding to approximately 60 % of the waves, but also seasonally, being higher during winter (about 65 %) and smaller during summer (about 55 %). Hence, waves that contribute with the erosion process are reaching the beach more frequently than the depositional ones for these areas, meaning that the seasonal variability could be important in the erosional capacity, but not in the general erosional trend. The high variability of stretch 6 and its presence in the shaded area might reduce the long-term effect of the erosion. Moreover, the proximity with an ebb-delta system and the transport trend toward NE could contribute to the maintenance of the sediment budget in this region, due to shoal attachment and sediment distribution along this area.

5 Conclusion

This study analyzed the wave climate, the wave power distribution, and the corresponding longshore drift gradients along the beach system of Ilha Comprida (SP). Although being based on numerical modeling results, due to the absence of in situ wave data, results provide important background information for the better understanding of erosion/accretion

processes along this stretch of exposed coast. The erosional spots can be explained by positive gradients in the potential longshore transport and the relative increase in local wave power, both seasonally and yearly. Thus, the wave power could have a large importance in long-term analysis, explaining variations in beach morphology combined with the longshore drift gradients. Furthermore, the wave power distribution and the wave characteristics along the entire system could be explained by the presence of the shaded area in the southern region and the coastline orientation, just as the spatial migration in the central-southern positive gradient trend. In addition, the central-northern region acts as a trap for the sediment coming from the SW, due to its depositional characteristics owing to negative longshore gradient and low relative wave power, thus contributing to the high erosion pattern at the northern sector, which, in addition to lower sediment supply, presents positive longshore drift gradients and increased wave power.

References

Araújo CES, Franco D, Melo E, Pimenta F (2003) Wave regime characteristics of the southern Brazilian coast. International Conference on Coastal and Port Engineering in Developing Countries, COPEDEC VI, Colombo, Sri Lanka, Proceedings. Paper 97. CD-ROM

Bird ECF (2008) Coastal geomorphology: an introduction. Wiley and Sons, Chichester, p 411

Bittencourt ACSP, Martin L, Dominguez JML, Silva IR, Sousa DL (2002) A significant longshore transport divergence zone at the northeastern Brazilian coast: implications on coastal quaternary evolution. An Acad Bras Cienc 74:505–518

Bittencourt ACSP, Dominguez JML, Martin L, Silva IR (2005) Longshore transport on the northeastern Brazilian coast and implications to the location of large scale accumulative and erosive zones: an overview. Mar Geol 219:219–234

Bush DM, Neal WJ, Young RS, Pilkey OH (1999) Utilization of geoindicators for rapid assessment of coastal-hazard risk and mitigation. Ocean Coast Manag 42:647–670

Cai F, Su X, Liu J, Li B, Lei G (2009) Coastal erosion in China under the condition of global climate change and measures for its prevention. Prog Nat Sci 19(4):415–426. doi:10.1016/j.pnsc.2008.05.034

Caires S, Sterl A, Bidlot JR, Graham N, Swail V (2004) Intercomparison of different wind-wave reanalyses. J Clim 17:1893–1913

Cassiano GF, Siegle E (2010) Migração lateral da desembocadura do Rio Itapocú, SC, Brasil: evolução morfológica e condicionantes físicas. Rev Bras Geofísica 28(4):537–549

Cipriani LE, Stone GW (2001) Net longshore sediment transport and textural changes in beach sediments along the southwest Alabama and Mississipi barrier islands, USA. J Coast Res 17:443–458

Conti LA, Araújo CAS, Paolo FS, Barcellos RL, Rodrigues M, Mahiques MM, Furtado VV (2012) An integrated GIS for sedimentological and geomorphological analysis of a lagoon environment. Barra de Cananéia inlet region, (Southeastern Brazil). J Coast Conserv 16(1):13–24

Davies JL (1980) Geographical variation in coastal development, 2nd edn. Longman, London, p 212

Davis Jr RA, Fitzgerald DM (2004) Beaches and coasts. Blackwell Publishing. Cap 6. p. 102-114

Folk RL, Ward WC (1957) Brazos river bar: a study in the significance of grain size parameters. J Sediment Petrol 27:3–26

Georgiou IY, Schindler JK (2009) Wave forecasting and longshore sediment transport gradients along a transgressive barrier island: Chandeleur Islands, Lousiana. Geo-Mar Lett 29:467–476. doi:10.1007/s00367-009-0165-3

Guedes CCF, Giannini PCF, Sawakuchi AO, Dewitt R, Nascimento Jr DR, Aguiar VAP, Rossi MG (2011) Determination of controls on Holocene barrier progradation through application of OSL dating: the Ilha Comprida Barrier example, Southeastern Brazil. Mar Geol 285(1):1–16

Harari J, Camargo R (1994) Simulação da propagação das nove principais componentes de maré na plataforma sudeste Brasileira através de modelo numérico hidrodinâmico. Boletim do Instituto Oceanográfico 42(1-2):35–54

Holthuijsen LH (2007) Waves in oceanic and coastal waters. Cambridge University Press, Cambridge, p 387

Holthuijsen LH, Booji N, Herbers THC (1989) A prediction model for stationary, short-crested waves in shallow water with ambient currents. Coast Eng 13:23–54

Italiani DM, Mahiques MM (2014) O registro geológico da atividade antropogênica na região do Valo Grande, Estado de São Paulo, Brasil. Quaternary Environ Geosci 05(2):33–44

Kawakubo FS (2009) Avaliação das Mudanças na Linha de Costa na Foz do Rio Ribeira de Iguape/Desembocadura Lagunar da Barra do Icapara (Litoral Sul de São Paulo - Brasil) Utilizando dados do Landsat *MSS*, *TM* e *ETM+*. Investigaciones Geográficas, Boletín del Instituto de Geografia, UNAM. 68: 41 – 49 pp

Komar PD (1998) Beach processes and sedimentation. 2nd edn. Prentice Hall

Marquez MRK, Mahiques MM (2010) Variações morfológicas no prisma praial da Ilha Comprida (Sudeste do Brasil)—Subsídios para uma Gestão Costeira Sustentável. Revista da Gestão Costeira Integrada 10(3):361–379

Martinho CT, Dillenburg SR, Hesp P (2009) Wave energy and longshore sediment transport gradients controlling barrier evolution in Rio Grande do Sul, Brazil. J Coast Res 25(2):285–293

Mesquita AR, Harari J (1983) Tides and tide gauges of Cananéia and Ubatuba—Brazil (Lat. 24°). Instituto Oceanográfico, Universidade de São Paulo, São Paulo, pp 1–14, Relatório, 11

Miller JK, Dean RG (2004) A simple new shoreline change model. Coast Eng 51(7):531–556

Nascimento Jr DR (2006) Morfologia e sedimentologia ao longo do sistema praia – duna frontal da Ilha Comprida, SP. Dissertação de mestrado. Instituto de Geociências. 155p

Pianca C, Mazzini PLF, Siegle E (2010) Brazilian offshore wave climate based on NWW3 reanalysis. Braz J Oceanogr 58(1):53–70

Pianca C, Holman R, Siegle E (2015) Shoreline variability from days to decades: results of long-term video imaging. J Geophys Res Oceans 120:2159–2178. doi:10.1002/2014JC010329

Santos SLC (2005) Um modelo de banco de dados geográficos para a resposta ao derramamento de óleo baseado na vulnerabilidade e sensibilidade do litoral paulista. Instituto Oceanográfico, Universidade de São Paulo, Tese de Doutorado, p 216

Short AD (1978) Wave power and beach stages: a global model. In: INTERNATIONAL CONFERENCE ON COASTAL ENGINEERING, 16. Hamburg, 1978. Proceedings. Hamburg, ASCE. pp. 1045-1062

Siegle E, Asp NE (2007) Wave refraction and longshore transport patterns along the southern Santa Catarina coast. Braz J Oceanogr 55 (2):109–120

Sousa PHGO (2013) Vulnerabilidade à erosão costeira no litoral de São Paulo: interação entre processos costeiros e atividades antrópicas. Tese de Doutorado. Instituto Oceanográfico da Universidade de São Paulo

Souza, CR de G (1997) As células de deriva litorânea e a erosão nas praias do Estado de São Paulo. Tese de Doutorado. Universidade de São Paulo, Instituto de Geociências, 2v

Souza CRG, Suguio K (1996) Coastal erosion and beach morphodynamics along the State of São Paulo (SE Brazil). An Acad Bras Cienc 68:405–424

Stive MJF, Aarninkhof SGJ, Hamm L, Hanson H, Larson M, Wijnberg KL, Nicholls RJ, Capobianco M (2002) Variability of shore and shoreline evolution. Coast Eng 47(2):211–235

Stone GW, JR Stapor FW, May JP, Morgan JP (1992) Multiple Sediment sources and a cellular, non-integrated, longshore drift system: Northwest Florida and Southwest Alabama coast. USA Marine Geol 105:101–154

Tessler MG (1988) Dinâmica sedimentar quaternária no litoral sul paulista. Tese de doutorado. Universidade de São Paulo, Instituto Oceanográfico. p 276

Tolman HL, Balasubramaniyan B, Burroughs LD, Chalikov DV, Chao YY, Chen HS, Gerald VM (2002) Development and implementation of wind-generated ocean surfacewave models at NCEP, vol 17. American Meteorological Society, Washington, D.C, pp 311–333

van Rijn LC (2011) Coastal erosion and control. Ocean Coast Manag 54: 867–887

Wang XLL, Swail VR (2001) Changes of extreme wave heights in Northern Hemisphere oceans and related atmospheric circulation regimes. J Clim 14:2204–2221

Zenkovich VP (1967) Processes of coastal development. Oliver & Boyd, Edinburgh, p 738